

## High resolution Near-field Fluorescence Microscopy: from principles to applications in cell biology

A. Cambi<sup>1</sup>, C. G. Figdor<sup>1</sup> and M.F. Garcia-Parajo<sup>\*2</sup>

<sup>1</sup>Department of Tumour Immunology, Nijmegen Center for Molecular Life Sciences, University Medical Center, Nijmegen, the Netherlands.

<sup>2</sup>BEC-Institut de Bioenginyeria de Catalunya, Barcelona Science Park (PCB), Josep Samitier, 1-5, 08028 Barcelona, Spain and ICREA-Institució Catalana de Recerca i Estudis Avançats, 08010 Barcelona, Spain.

The ability to study the structure and function of cell membranes is fundamental to understanding cellular processes. This requires the use of methods capable of resolving structures with nanometre-scale resolution in intact or living cells. Although fluorescence microscopy has proven to be an extremely versatile tool in cell biology, its diffraction-limited resolution prevents the investigation of membrane compartmentalisation at the nanometre scale. Near-field scanning optical microscopy (NSOM) is a relatively unexplored technique that provides optical resolution below 100nm enabling the visualisation of nano-scale domains on the cell membrane with single molecule detection sensitivity at physiologically relevant packing densities in *aqueous* conditions. In this contribution we discuss the implementation of NSOM and illustrate its unique advantages in terms of spatial resolution, sensitivity and surface specificity for the study of protein clustering at the cell membrane.

**Keywords** high-resolution optical microscopy; near-field optical microscopy (NSOM); single molecule detection; cell membrane compartmentalisation.

### 1. Introduction

Conventional optical microscopy and in particular fluorescence microscopy have become one of the most prominent and versatile research tools used in modern cell biology [1]. On the one hand, light-based microscopy allows the study of living specimens in their native environment in a non-invasive manner. Additionally, fluorescence microscopy offers chemical specificity by exploiting polarisation, lifetime and spectral contrast [2]. Furthermore, progress in detector technology has recently pushed fluorescence microscopy to its ultimate level of sensitivity: the detection of individual molecules [3-5]. At the same time, enormous progress on the development of specific and highly efficient fluorescent probes for exogenous labelling has been achieved. In parallel to external antibody labelling, the advent of green fluorescent protein (GFP) technology has revolutionised live cell imaging because an autofluorescent molecule can be genetically encoded as a fusion with the c-DNA of interest [6]. The spectral variants of GFP and the unrelated red fluorescent protein (DsRed) make it possible to perform multicolour imaging in living cells [6,7].

In the last few years, a number of optical-based techniques have been applied to study the organisation of the cellular plasma membrane with single molecule detection sensitivity. Figure 1 illustrates some of the most commonly used approaches. In total internal reflection microscopy (TIRF) (Fig. 1*a,b*) an evanescent field is created at the interface between the glass substrate and the cell surface. Because the excitation intensity decays exponentially as a function of the distance from the glass-cell interface, TIRF allows selective excitation at the cell membrane. The technique is widely used for single molecule detection and has the capability of monitoring dynamic processes with high time resolution [8]. Unfortunately, only the membrane-glass interface is effectively illuminated, a region where most probably dynamical processes are hindered by the presence of the glass substrate. Furthermore, the lateral resolution in TIRF is limited to length scales > 300 nm, lacking the spatial resolution necessary to

\* Corresponding author: e-mail: mgarcia@pcb.ub.es, Phone: +34 934039615

probe nano-scale organisation of membrane components. In scanning confocal microscopy (Fig. 1c) the detection volume is reduced by using a pinhole that rejects out-of-focus light and enables imaging of thin sections of the cell, in particular the cell membrane. Nevertheless, the lateral resolution is still diffraction limited and since the penetration depth in the axial direction is in the order of the wavelength used, background from cellular autofluorescent components is a problem for single molecule detection. Recently, 4Pi and stimulated emission depletion microscopy have been developed with the aim of improving the lateral resolution of confocal microscopy [9,10]. Both techniques have demonstrated increased lateral and axial resolution, although broad applicability still needs to be shown convincingly. A successful and widely applied method to gain contrast at the nanometre scale is fluorescence resonance energy transfer (FRET) [11]. The efficiency of the energy transfer process is strongly dependent on the fluorophores distance separation ( $r^{-6}$ ) and thus ideally suited to investigate proximity and interactions between proteins in the 1-10nm spatial scale [11]. Thus, while diffraction limited methods are able to visualise structures larger than 300nm, FRET focuses on processes occurring at distances smaller than 10nm, leaving behind a considerable and important spatial gap inaccessible to optical investigation.

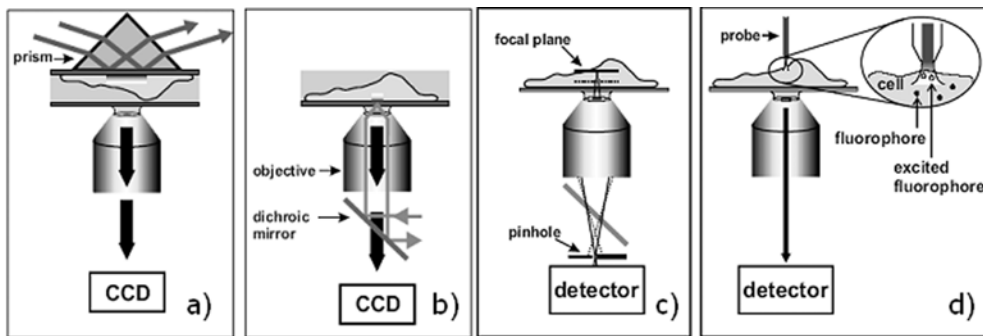


**Fig. 1** Schematics of the different experimental schemes to investigate the organisation of the cellular plasma membrane; *a, b*) Total internal reflection microscopy relies on an evanescent field at the interface between glass and the cell surface. Two practical configurations are normally used to generate the evanescent field, i.e., *a*) via a prism, or *b*) using the edges of a high NA objective. The objective collects the fluorescence, which is filtered from the excitation light and detected by a two dimensional array detector, usually a CCD camera; *c*) In confocal microscopy the excitation light is focused onto the sample. Fluorescence from the focal plane (solid line) and from out-of-focus regions (dotted line), is collected by the same objective, filtered and detected by an avalanche photodiode (APD). Out-of-focus light is rejected by using a pinhole in front of the detector; *d*) In near-field scanning optical microscopy a subwavelength aperture probe illuminates the upper part of the cell membrane. Fluorescence is collected in the far-field using a high NA objective, filtered and detected with an APD.

Near-field scanning optical microscopy (NSOM) is a promising optical technique able to bridge this gap by bringing spatial resolution down to the level of several tens of nanometres. This chapter focuses on the application of NSOM to investigate, with single molecule detection sensitivity, the lateral organisation of the cell membrane in intact cells with a spatial resolution better than 100 nm. We will show the suppression of autofluorescence background when imaging the cell membrane, facilitating the visualisation of nano-scale protein domains. Furthermore, we will discuss the added value of combining single molecule detection sensitivity with high spatial resolution for discriminating monomer *vs.* clustered organisation of membrane receptors. Finally, we will demonstrate that NSOM is capable of routine operation in an *aqueous* environment, enabling the study of the cell membrane in native conditions, opening new ways to investigate the relation between membrane organisation and cell function.

## 2. Near-field scanning optical microscopy (NSOM)

NSOM is a technique that preserves the advantages of the evanescent type of illumination, while providing simultaneously lateral resolution beyond the diffraction limit of light. The technique (Fig. 1d) is based on scanning a small subwavelength aperture probe in close proximity to the sample surface. The lateral resolution, down to tens of nanometres, is essentially defined by the size of the aperture and the sample-to-probe distance. The probe illuminates the sample with an evanescent field that is strongly localised at the vicinity of the aperture and decreases very rapidly away from the probe's end face [12,13]. Due to the exponentially decaying character of the illumination field, NSOM is a surface sensitive technique, and it is therefore ideal for studying the cell membrane [14,15]. In addition to its surface sensitivity, NSOM provides simultaneous topographic and fluorescence imaging [12-14,16]. Finally, the small excitation volume ( $10^5 \text{ nm}^3$  versus  $10^8 \text{ nm}^3$  as obtained in confocal microscopy) reduces dramatically cytoplasm background fluorescence enabling single molecule detection on the cell membrane [14] with a high signal-to-background ratio.

Despite its apparent advantages, the application of NSOM in biology has witnessed a modest progress. Successful examples on cell membrane studies include the co-localisation of proteins within the membrane of malaria parasite-infected red blood cells at a resolution of  $\sim 100 \text{ nm}$  [17], mapping the clustering of major histocompatibility complexes I and II in fibroblast cells [18], identification of membrane lipid and proteins on fibroblast [19] and the study of ion channel clusters in cardiac myocyte membranes [20]. More recently, we have used the technique to investigate the nano-scale organisation of C-type lectins on the membrane dendritic cells, both under dry and liquid conditions [21,22].

Figure 2 shows the schematics of the combined confocal/NSOM microscope routinely used in our experiments. The experimental set-up is integrated into an inverted optical microscope (Zeiss Axiovert 135TV). The microscope has access to two  $\text{Ar}^+/\text{Kr}^+$  ion lasers, providing a wide wavelength range (457nm – 647nm). Laser light enters the set-up via two optical paths where adjustment of the beam width, excitation intensity and polarisation are controlled independently. Both beams are then combined by a beam splitter. In confocal mode, the light is guided through a short piece of single mode fibre that acts as a spatial filter, guaranteeing full overlay of the two wavelengths. After a beam expander, the incoming circularly polarized light is reflected by a dichroic mirror and focused onto the sample using an oil-immersion objective (Olympus,  $64\times$ , 1.4 NA). In the NSOM mode, single or dual excitation light is coupled into an Al-coated tapered fibre probe. A flipable mirror mount enables easy switching between confocal and NSOM excitation modes. On the detection side, the emitted fluorescence is collected by the objective and selected using appropriate long-pass filters. The fluorescence is then separated in two channels, with either polarisation or spectral contrast, and focused onto two single photon counting avalanche photodiodes.

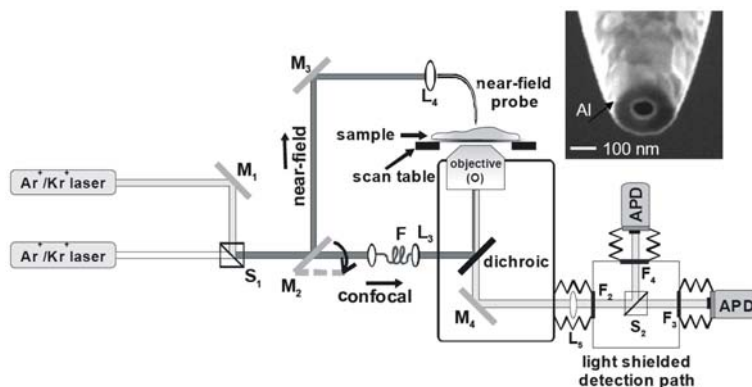


**Fig. 2** Schematics of the combined confocal/NSOM set-up. The inset shows a 70nm diameter NSOM probe. The aperture primarily determines the optical resolution of the microscope. Because of the evanescent character of the light exiting the probe, the optical near-field excitation has significant intensity only in a layer of  $<70\text{nm}$  away from the aperture. This means that lower-lying fluorophores are not excited, resulting in an effective suppression of background fluorescence.

One of the crucial aspects of NSOM relies on the fabrication of reproducible aperture probes. Our probes are based on single mode optical fibres, fabricated using the “heating and pulling” method, followed by an Al deposition layer ( $\sim 100\text{nm}$ ) in order to confine the light within the probe (see inset in Fig. 2) [23]. Typical diameters are 70-100nm with throughput efficiency of  $10^{-5}$ - $10^{-4}$ , depending on the aperture size [23]. The probe is kept in the near-field region of the sample ( $< 10\text{ nm}$ ) by means of a shear-force feedback based on a piezo-electric element, providing simultaneously a topographic map of the sample surface while scanning [13,14,16]. To increase the versatility of the system, we have recently developed a reliable and easy-to-use system, with perfect analogy to a diving bell, to allow NSOM operation under *aqueous* conditions [24]. A small glass tube carefully glued into an aluminium holder encapsulates the piezo-electric element, so that vibration is performed in air. A small part of the NSOM probe protrudes out of the glass tube and is in contact with the wet sample. Using this concept we have shown that NSOM is able to operate in liquid environments without compromising resolution or sensitivity [24].

### 3. High resolution single molecule imaging using NSOM

To demonstrate the potential of NSOM as a high-resolution optical technique to study the organisation of proteins on the cell membrane, we have imaged the integrin receptor LFA-1 expressed on the membrane of stably transfected fibroblasts (L-cells). Figure 3a shows a bright field image of an L-cell stretched on PLL coated-glass, while Fig. 3b,c show the simultaneously obtained topography and near-field fluorescence image respectively, of the part highlighted in Fig. 3a. The fluorescence image shows clearly defined spots that correspond to the emission of individual GFP proteins fused to the  $\beta$ -chain of LFA-1. Individual molecules are recognised by their distinct properties such as discrete photobleaching and blinking [5], some of them pointed out by the arrows in Fig. 3c. The size of the spots is about 70 nm, which roughly corresponds to the diameter of the NSOM probe used in these experiments. In addition, it is important to note that the shallow penetration depth of the illumination field emanating from the NSOM probe results in a large suppression of the cell autofluorescence background and GFP signal from the cytoplasm. As such, the technique allows discriminating with high single-to-noise ratio single molecules exclusively on the cell membrane.

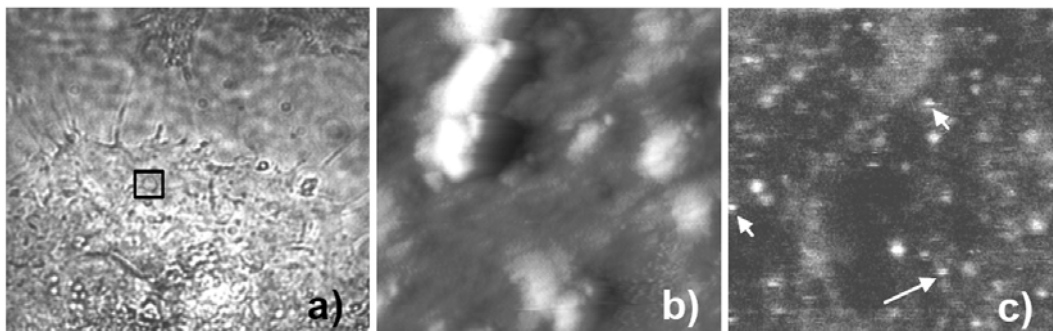


**Fig. 3** Near-field fluorescence imaging of GFP-LFA-1 on L-cells; *a)* Bright field image of an L-cell stretched on PLL-coated glass. The image is  $50\mu\text{m}^2$  in size. A small part of the membrane, indicated by the square box is then scanned with NSOM; *b)* topography and *c)* simultaneously obtained near-field fluorescence image. The size of the images is  $3.2\mu\text{m}^2$ , with 256x256 pixels. Arrows in *c)* point to some single GFP emission spots.

Due to its single molecule sensitivity and enhanced resolution, NSOM is also capable to quantify the degree of protein clustering at the cell membrane at physiologically relevant packing densities. As an example, Fig. 4a shows a combined topography and near-field fluorescence image (bright spots) of the HIV-1 receptor DC-SIGN expressed on an immature dendritic cell (imDC). In this case, DC-SIGN has been externally labelled via antibodies conjugated to the fluorophore Cy5. The cell height on the dentrite region varied from tens of nm to 250nm approximately, as measured from the topographic image,

confirming that the cell is well stretched on the substrate. The combination of topography and fluorescence intensity also allows the determination of the absolute position of fluorescent spots on the membrane. As seen from the image, numerous fluorescent spots decorate the membrane. The fluorescence spots vary in size and brightness, indicating emission from multiple fluorophores per spot and thus protein clustering.

#### 4. Quantitative analysis derived from NSOM images

Although from a first inspection of the NSOM images a qualitative impression on the spatial organisation of protein components on the cell membrane is readily obtained, more quantitative insight on their organisation can be gained by analysing the fluorescence spots in terms of their intensity, size and relative position on the cell surface. The total number of detected photon counts from a spot is directly related to the number of fluorophores and thus to the number of proteins, depending on the antibody labelling efficiency. As observed from Fig. 4a the fluorescence varies from spot to spot, indicating a wide spread on the number of proteins involved in each spot. For the fluorescence intensity analysis we integrate all photon counts within a contour of ~15% of the peak intensity of a given spot, subtract the background from a similar area in the vicinity of that spot and finally divide by the total fluorescence acquisition time of the spot. A histogram containing the intensity of more than 1000 spots analysed from multiple NSOM images is shown in Fig. 4b. The spot intensities range from less than 5 kcounts/s to 1000 kcounts/s, indicating a large spread on the number of Cy5 dyes per spot. The low intensity part of the total histogram is expanded in the inset of Fig. 4b, which also includes the distribution of intensities that solely correspond to single molecule spots. The peak of the single molecule intensity histogram (~7 kcounts/s) is then used to normalise the total intensity distribution in terms of the number of Cy5 molecules. The overall intensity distribution peaks at ~3.5 Cy5 molecules with an average value of ~30 Cy5 molecules. Considering an antibody-DC-SIGN binding efficiency of 0.5-1, and antibody labelling efficiency of ~3 Cy5 per secondary antibody, as determined from independent single molecule antibody experiments, these results indicate that the average number of DC-SIGN molecules contained in a cluster is ~5-10 [21]. Moreover, the overall intensity distribution demonstrates that as much as 80% of DC-SIGN is clustered on the membrane, each cluster hosting from a few to several tens of DC-SIGN molecules. It is important to mention that clustering of DC-SIGN was observed in all analysed images (20 independent NSOM measurements over seven representative cells) obtaining similar variability in terms of cluster intensity. These results are also in agreement with Transmission Electron Microscopy (TEM) data previously obtained on imDCs [25].

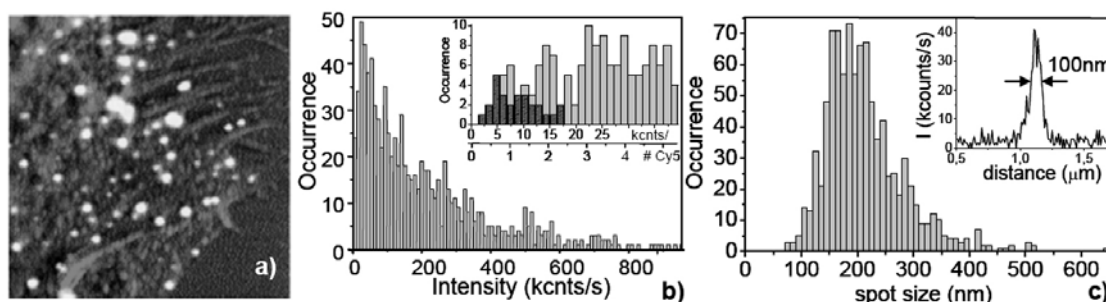


**Fig. 4** DC-SIGN externally labelled with Cy5 on an immature DC. Cells were first stretched on fibronectin-coated glass, labelled with antibodies, fixed with 1% PFA, dehydrated, and critical-point dried; *a*) Combined topography and near-field fluorescence image. The image is  $7\mu\text{m}^2$ . The topography image clearly shows some of the dendrites of the cell (height of 20nm) while fluorescence spots of different intensity and size decorate the cell surface; *b*) Intensity distribution on 1200 individual spots obtained over multiple NSOM images. The inset shows a zoom-in on the lowest intensity values of the distribution (<40 kcounts/s), together with the intensity of single molecule spots (shaded histogram); *c*) Spot size distribution (FWHM) of 1200 different measured spots. The intensity profile through a single molecule spot is shown in the inset.

Further evidence for protein clustering is obtained by measuring the physical size of each fluorescent spot. The size is determined by fitting the measured intensity profile with a 2D Gaussian function. The spot size is then defined as the full-width at half-maximum (FWHM) of the fit. A histogram of spot sizes as obtained from imaging DC-SIGN using NSOM is shown in Fig. 4c. The spot sizes vary from 70 to 650 nm with a peak at 200 nm. The inset in Fig. 4c shows the FWHM of a single molecule fluorescent spot reflecting the size of the aperture probe, and being clearly below the peak of the distribution. Noticeably, the size of the clusters is below the diffraction limit of light and therefore not accessible by standard optical means. The high spatial resolution of NSOM is therefore crucial to directly resolve the physical size of nanometric-sized domains on the cell membrane without the need of de-convolution algorithms.

## 5. High resolution NSOM imaging in liquid

The most technical challenge associated with the use of NSOM for biological research concerns the difficulty of operating the technique in physiological relevant conditions. Although important biological information can be extracted from NSOM on dry biological samples, these results are always subject to potential drying artefacts. We have recently shown that the performance of NSOM can be extended to measurements in liquid environments using a diving bell concept [24], and showed for the first time single molecule detection sensitivity with 90nm spatial resolution on wet cells [22].

To demonstrate the general applicability of NSOM for cell membrane studies in liquid conditions, we have extended our investigation of the organisation of DC-SIGN to wet dendritic cells. Figure 5a shows the confocal image of a large region of a DC expressing DC-SIGN on the surface, while Figs. 5b and 5c show the simultaneously obtained topographic and near-field image of a highlighted region of the membrane. As clearly observed from the NSOM image, operation in *aqueous* conditions is successfully achieved with similar sensitivity and resolution as obtained on dried material. The topographic image in Fig. 5b serves as a mask to identify the contours and the cell region, excluding any possible fluorescence miss-assignment due to unspecific binding of antibodies to the glass substrate.

A further zoom-in of the cell membrane is shown in Fig. 5d where well-separated DC-SIGN domains are clearly visible. The line traces through two different clusters in Figs. e and f demonstrate the superior resolution of NSOM with respect to the diffraction limited resolution of confocal microscopy. The FWHM of a Gaussian fit to the fluorescence profiles render values of 90nm and 120 nm for the line traces shown in Fig. 5e and f respectively. The difference in intensity ( $9 \times 10^4$  and  $1.6 \times 10^5$  counts/s for e and f respectively) indicates that a different number of proteins are involved in both domains. Thus, clustering of DC-SIGN is also apparent in these images, consistent with our previous observations using TEM [25] and NSOM [21] on dried DCs, and confirming that indeed DC-SIGN is organised into sub-diffraction limit sized domains in the membrane of immature DCs.

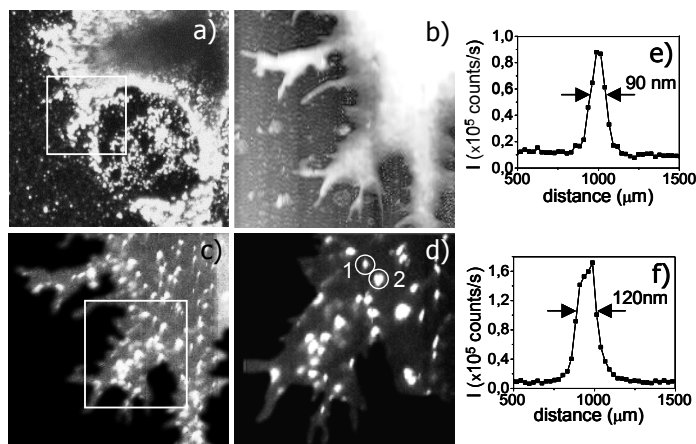


**Fig. 5:** a) Fluorescence image of DC-SIGN on an imDC in buffer solution collected in confocal mode ( $32 \mu\text{m}^2$ ). Samples were prepared in a similar fashion as for Fig. 5, but without the dehydration and critical point dry steps. Simultaneously obtained b) topography and c) NSOM image ( $16.5 \mu\text{m}^2$ ) of the highlighted area in a); d) zoom-in NSOM image ( $7 \mu\text{m}^2$ ) of the area highlighted in c); e) and f) show line traces along the two clusters encircled in d), demonstrating the high spatial resolution of NSOM.

## 6. Conclusions and outlook

In this contribution we have provided examples on the applicability of near-field scanning optical microscopy for studying the heterogeneity and lateral organisation of the cell membrane both on dried and *aqueous* conditions. NSOM combines the high resolution of scanning probe microscopy with the contrast of optical microscopy. Single molecule detection sensitivity combined with high spatial resolution allows quantitative differentiation between monomer *vs.* clustered type of organisation. Furthermore, the small excitation volume of NSOM allows independent observation of individual molecules at physiological relevant packing densities, which is more than one order of magnitude higher than achieved by confocal or wide field imaging [26].

Until recently, technical difficulties when operating NSOM in liquid conditions have restricted its use to fixed, dried cells, hampering its broad applicability in the biological community. We have now demonstrated that NSOM can be reliably operated in physiological conditions using a simple concept, opening the way to high-resolution live cell imaging. However, one must be aware that as scanning probe technique, NSOM is inherently slow, being less suitable for monitoring lateral diffusion processes of membrane complexes. On the other hand, its excellent axial resolution should allow for the monitoring of exo- and endo-cytosis processes with high speed and sensitivity.

Co-localisation studies, a common application of far-field fluorescence imaging in cell biology, when performed with NSOM should provide unprecedented detail and accuracy which are impossible to obtain by diffraction-limited imaging techniques. One of added advantages of illuminating via the NSOM probe is the overlay of two or more excitation wavelengths to the same nanometric sized excitation source, eliminating chromatic aberrations inherent to lens-based microscopy. In this context, we are currently using two-colour excitation NSOM in *aqueous* conditions to investigate the association of specific membrane proteins to lipid rafts. Until now, possible association between lipid rafts and proteins have been studied using biochemical methods in combination with confocal techniques based on co-patching [27]. In the years to come, NSOM will certainly become an important nanotool in cell biology, contributing to the understanding of the current model for the micro- and nano-scale organisation of the cellular plasma membrane.

**Acknowledgements** The authors would like to thank B.I. de Bakker and M. Koopman for the NSOM images presented here. B. Joosten is gratefully acknowledged for sample preparation & fruitful discussions. AC is supported by NWO VENI grant 916.66.028 from the Netherlands Organization of Scientific Research. Support by Netherlands Technology Foundation (STW) Netherlands Foundation for Fundamental Research of Matter (FOM) is gratefully acknowledged.

## References

- [1] D.J. Stephens and V.J. Allan, *Science* **300**, 82 (2003).
- [2] X. Michalet, A.N. Kapanidis, T. Laurence, F. Pinaud, S. Doose, M. Pfugheofft, S. Weiss, *Annu. Rev. Biophys. Biomol. Struct.* **32**, 161 (2003).
- [3] E. Betzig and R.J. Chichester, *Science* **262**, 1422 (1993).
- [4] W.E. Moerner and M. Orrit, *Science* **283**, 1670 (1999).
- [5] M.F. Garcia-Parajo, J.A. Veerman, R. Bouwhuis, R. Vallee and N.F. van Hulst, *ChemPhysChem*, **2**, 347 (2001).
- [6] R.Y. Tsien, *Annu. Rev. Biochem.* **67**, 509 (1998).
- [7] J. Lippincott-Schwartz and G.H. Patterson, *Science* **300**, 87 (2003).
- [8] Y. Sako and T. Yanagida, *Nat. Cell Biol. Supl.* **S**, SS1. (2003)
- [9] S.W. Hell and E.H. Stelzer, *J. Opt. Soc. Am.* **9**, 2159 (1992).
- [10] T.A. Klar, S. Jakobs, M. Dyba, A. Egner and S.W. Hell, *Proc. Natl. Acad. Sci. USA* **97**, 8206 (2000).
- [11] E.A. Jares-Erijman and T.M. Jovin, *Nat. Biotech.* **21**, 1387 (2003).
- [12] E. Betzig and J.K. Trautman, *Science* **257**, 189 (1992).

- [13] M.A. Paesler and P.J. Moyer, Near-field optics, theory, instrumentation and applications. Wiley-Interscience ISBN 0471043117 (1996).
- [14] F. de Lange, A. Cambi, R. Huijbens, B. I. de Bakker, W. Rensen, M. F. Garcia-Parajo, N.F. van Hulst and C.G. Figdor, *J. Cell Sci.* **114**, 4153 (2001).
- [15] T.A. Laurence and S. Weiss, *Science* **299**, 667 (2003).
- [16] N.F. van Hulst, M.F. Garcia-Parajo, M.H.P. Moers, J.A. Veerman and A.G.T. Ruiter, *J. Struct. Biol.* **119**, 222, (1997).
- [17] Th. Enderle, T. Ha, D.F. Ogletree, D.S. Chemla, C. Magowan and S. Weiss *Proc. Natl. Acad. Sci. USA.* **94**, 520 (1997).
- [18] P. Nagy, L. Matyus, A. Jenei, G. Pany, S. Varga, J. Matko, J. Szollosi, R. Gaspar, T.M. Jovin, and S. Damjanovich, *J. Cell Sci.* **114**, 4153 (2001).
- [19] J. Hwang, L.A. Gheber, L. Margolis and M. Edidin, *Biophys. J.* **74**, 2184 (1998).
- [20] A. Ianoul, D. Grant, Y. Rouleau, M. Bani-Yaghoub, L. Johnston and J. P. Pezacki, *Nat. Chem. Biol.*, **1**, 196 (2005).
- [21] B.I. de Bakker, F. de Lange, A. Cambi, J.P. Korterik, E.M.H.P. van Dijk, N.F. van Hulst, C.G. Figdor, and M.F. Garcia-Parajo, *ChemPhysChem*, in press (2007).
- [22] M. Koopman, A. Cambi, B.I. de Bakker, B. Joosten, C.G. Figdor, N.F. van Hulst and M.F. Garcia-Parajo, *FEBS Lett.* **573**, 6 (2004).
- [23] J.A. Veerman, A.M. Otter, L. Kuipers and N.F. van Hulst, *Appl. Phys. Lett.* **72**, 3115 (1998).
- [24] M. Koopman, B.I. de Bakker, M.F. Garcia-Parajo and N.F. van Hulst, *Appl. Phys. Lett.* **83**, 5083 (2003).
- [25] A. Cambi, F. de Lange, N. M. van Maarseveen, M. Nijhuis, B. Joosten, E. M. H. P. van Dijk, B. I. de Bakker, J. A. M. Fransen, P. H. M. Bovee-Geurts, F. N. van Leeuwen, N. F. van Hulst, C. G. Figdor, *J. Cell Biol.* **164**, 145 (2004).
- [26] M. Vrljic, S.Y. Nishimura, S. Brasselet, W.E. Moerner and H.M. McConnell, *Biophys. J.* **83**, 2681 (2002).